https://doi.org/10.5194/angeo-2020-93
Preprint. Discussion started: 21 January 2021

Annales Geophysicae Discussions

Influence of different types of ionospheric disturbances on GPS signals at polar latitudes

Vladimir B. Belakhovsky[1], Yaqi Jin[2], Wojciech J. Miloch[2]

[1] Polar Geophysical Institute, Apatity, Russia
[2] Department of Physics, University of Oslo, Oslo, Norway

Correspondence to: Vladimir B. Belakhovsky (belakhov@mail.ru)

Abstract. The comparative research of the influence of different types of auroral particle precipitation and polar cap patches (PCP) on the GPS signals disturbances in the polar ionosphere was done. For this purpose, we use the GPS scintillation receivers at Ny-Ålesund and Skibotn, operated by the University of Oslo. The presence of the auroral particle precipitation and polar cap patches was determined by using data from the EISCAT 42m radar on Svalbard. The optical aurora observations in 557.7 nm, 630.0 nm spectrum lines on Svalbard were used as well for the detection of ionospheric disturbances. The cusp identification was done with using SuperDARN (Hankasalmi) data.

We consider about 150 events when the simultaneous EISCAT 42m and GPS data were available for the 2010-2017 years, in paper we present in detail only typical examples describing the overall picture. It was considered the dayside/cusp precipitation, substorm precipitations, daytime and nighttime PCP, precipitation associated with the interplanetary shock wave arrival. Cusp phase scintillations are lower than dayside PCP scintillations. We demonstrate that substorm-associated precipitations (even without PCP) can lead to a strong GPS phase (σ_ϕ) scintillations up to ~2 radians which is much stronger than those usually produced by other types of the considered ionosphere disturbances. At the same PCPs can lead to stronger ROT (rate of total electron content) variations. So our observations suggest that the substorms and PCPs, being different types of the high-latitude disturbances, lead to the development of different types and scales of ionospheric irregularities.

1. Introduction

The Global Navigation Satellite Systems (GNSS) have a great influence on human society today. The ionosphere as a medium for the radio waves propagation can produce a negative impact on the quality of the received signal. Global Positioning System (GPS) uses two frequencies: $f1$ = 1575.42 MHz and $f2$ = 1227.60 MHz. There are a lot of dual frequency GPS receivers all over the world which are used for the ionosphere studies. Irregularities in the plasma density can lead to rapid fluctuations of amplitude and phase of the signal which is referred to as ionosphere scintillations [Basu et al., 2002].

https://doi.org/10.5194/angeo-2020-93
Preprint. Discussion started: 21 January 2021


Annales Geophysicae Discussions

Strong scintillations reduce the quality of the signal and even lead to the signal loss. Thus, the investigation of GPS scintillations is an important aspect of space weather. The level of scintillations is characterized by the phase ($\sigma\Phi$) and amplitude (S4) scintillation indices. Amplitude scintillations are caused by the plasma irregularities with scale sizes ranging from tens to hundreds of meters, while the phase scintillations are caused by the irregularities with the sizes from hundreds of meters to several kilometers. Ionospheric scintillations are most severe in the equatorial region and at high latitudes [Basu et al., 2002; Kintner et al., 2007].

The high-latitude ionosphere is very dynamic and unpredictable structure forming plasma irregularities on a wide variety of scale sizes (from 1000 km to decameter scale). Case studies have indicated a relationship between auroral appearance and GPS scintillations [Smith, 2008; Prikryl et al., 2010, Kinrade et al., 2013]. Mostly discrete aurora cause strong scintillations and cycle slips (i.e. jump in differential phase TEC). Phase scintillation is more prominent than amplitude scintillation in the polar ionosphere [Prikryl et al., 2010]. Ionospheric phase disturbances over auroral region are frequent phenomena which often occur during night time [Prikryl et al., 2011].

One of the most dynamic ionospheric disturbances at high latitudes is the substorm. Magnetosphere substorm is a transient process originated on the nightside of the Earth, when a significant amount of energy derived from the solar wind-magnetosphere interaction is stored in the in the magnetosphere tail and then realized into the auroral ionosphere [Rostoker et al., 1980]. The substorms are characterized by the sporadic precipitation of energetic electrons from the magnetotail that leads to the appearance of the bright aurora. GPS signal phase correlate well with substorm-associated auroral disturbances.

It was found that polar moving auroral forms (PMAF) which are discrete auroral forms produced by the transient magnetopause reconnection have big impact on GNSS phase scintillations [Oksavik et al., 2015]. Authors found that the scintillation impact is strongest when PMAFs are in coincidence with PCP. Studies of [Van der Meeren et al., 2016] showed the sun-aligned arc in the polar cap does not cause significant phase scintillations. At polar latitudes polar cap patches have produce severe ionosphere disturbances. Polar cap patches are 100–1000 km islands of enhanced F-region plasma density. The patches are appeared near the cusp and then propagate along the ionospheric convection streams into the nightside auroral oval modulated by the nightside tail reconnection, after that patches returned to the dayside [Lockwood and Carlson, 1992; Zhang et al., 2013]. During strong and stable polar cap convection, segmentation may not happen and a continuous tongue of ionization (TOI) may be formed across the polar cap [Foster et al., 2005]. Phase scintillations in TOI were studied in the paper [Van der Meeren, 2014], it was observed bursts of phase scintillation and no amplitude scintillation in relation to the leading gradient of the TOI. Patches may develop smaller-scale irregularities down to decameter scale through the Kelvin-Helmholtz (KH) and gradient drift instabilities [Oksavik et al., 2012; Clausen et al., 2016]. In the auroral oval, polar cap patches are termed auroral blobs [Lorentzen et al., 2010]. Several types of auroral blobs are selected in previous investigations: boundary blobs, subauroral blobs, and auroral blobs [Crowley et al., 2000]. These airglow emissions are detectable from ground optical instruments as structures propagating from high to low latitudes.

Statistical studies found one peak in the occurrence rate of GPS phase scintillation around magnetic noon and another peak around magnetic midnight [Jin er al., 2015]. It is also found that the phase scintillation occurrence rate is higher in the

https://doi.org/10.5194/angeo-2020-93
Preprint. Discussion started: 21 January 2021


Annales Geophysicae Discussions

dayside, while the strong phase scintillation occurs more frequently during night. Nonetheless, strong phase scintillation events can also be triggered at daytime in association with the PMAF.

Jin et al. (2014) found that polar cap patches have their biggest impact on GPS signals once they reach the nightside auroral oval, in particular when combined with upward field-aligned currents [Clausen et al. 2016]. Jin et al. [2014] focused on phase scintillation measurements inside polar cap patches identified in airglow imager data and found that patches have a moderate scintillation impact ($\sigma\phi$~0.2). They also found, however, that the strongest impact on scintillations occurred when these patches cross from the polar cap into the auroral oval to become auroral blobs [Jin et al., 2016]. It was shown in the paper [Jin et al., 2014; Jin et al., 2016] that PCP can produce GPS scintillations quite comparable with scintillations during the particle precipitation with appearance of strong green aurora. But it was a case study therefore this question needs further studies.

The high-latitude disturbances have a great negative influence of radio propagation. So it is important to know what type of the high-latitude ionosphere disturbances has strongest influence on GPS navigation systems. In the present work we address the following question: what disturbances in the polar ionosphere (particle precipitation or polar cap patches) have stronger impact on the scintillations of GPS signals?

2. Instruments

The Ny-Ålesund (NYA) GPS scintillation receiver of the University of Oslo (UiO) was the main instrument used in our study. Upon availability of data, the Skibotn (Norway, mainland) GPS receiver was also used. The UiO GNSS scintillation receiver is the standard GNSS Ionospheric Scintillation/total electron content (TEC) Monitor (GISTM), model GSV4004B [Van Dierendonck et al., 1993]. The carrier phase and power at the L1 frequency (1.57542 GHz) are tracked and recorded at 50 Hz rate. The phase ($\sigma\phi$) and amplitude scintillation indices (S4) are also calculated and recorded automatically. The phase scintillation index is defined as the standard deviation of the carrier phase that has been detrended by the high-pass sixth-order Butterworth filter with a cutoff frequency of 0.1 Hz. The amplitude scintillation index (S4) is defined as the standard deviation of the received signal power, based on the 50-Hz sampling rate, normalized to the average signal power over one minute periods. The phase scintillation index is defined as the standard deviation of the carrier phase that has been detrended by a high-pass sixth-order Butterworth filter that were computed over one minute intervals are used in this study.

The GPS TEC data have been postprocessed by using WinTEC-P [Carrano et al., 2009]. The ROT (Rate of TEC) data over 1 min are also used to depict the TEC variations [see, e.g., Alfonsi et al., 2011], where ROT = ΔTEC/Δt.

For the describing the ionospheric plasma parameters (density, ion and electron temperature, line of sight ion velocity as a function of range) we used the Svalbard EISCAT 42m radar and UHF radar in Tromsø. The beam of the EISCAT 42m radar is directed along the geomagnetic field (azimuth = 184°, elevation = 82°). The UHF radar beam was fixed at an azimuthal angle of 185˚ and elevation angle of 77˚ (i.e., in the field-aligned direction in the F region).

https://doi.org/10.5194/angeo-2020-93
Preprint. Discussion started: 21 January 2021


Annales Geophysicae Discussions

For some convenient cases the optical aurora observations by all-sky imager of University of Oslo, Polar Geophysical Institute on Svalbard was used. The ASI in Ny-Ålesund (named NYA4) was located at Sverdrup Research Station. The NYA4 ASI used an EMCCD (electron multiplying charge-coupled device). Imager record emission intensity across the sky with a 180° field of view fish eye lens at 630.0 nm every 30 s and 557.7 nm every 15 s, respectively. The intensity of ASI is calibrated into the standard kilo Rayleigh (kR) intensity scale.

The stations mentioned in this study have the following geographic and geomagnetic (CGM) coordinates:

Ny Ålesund (NYA) – [78.92°N, 11.95°E], [75.25°N, 112.08°E];

Longyearbyen (LYR) – [78.20°N, 15.82°E], [75.12°N, 113.00°E];

Hornsund (HOR) – [77.00°N, 15.60°E], [74.13°N, 109.59°E];

Tromsø (TRO) – [69.66°N, 18.94°E], [66.64°N, 102.90°E];

Skibotn (SKN) – [69.43°N, 20.38°E], [66.28°N, 103.41°E].

IMAGE magnetometer data was used for the geomagnetic field observations. OMNI database was used for the evaluating the solar wind and interplanetary magnetic field parameters. We use the 1 min resolution Sym-H index and AE indices to show the geomagnetic storm and substorm activity. The Sym-H and AE indices were obtained from the World Data Center for Geomagnetism at Kyoto University (http://wdc.kugi.kyoto-u.ac.jp/).

3. Analysis of ionosphere disturbances

In the present study, we considered the influence of different geophysical phenomena on the GPS scintillations: dayside/cusp precipitation, nighttime substorm precipitation, daytime and nighttime polar cap patches, precipitations associated with the interplanetary shock arrival. We focused mainly on the phase scintillation index because amplitude scintillation index (S4) practically has no large variations t high latitudes. The presence of the particle precipitation into the ionosphere associated with the appearance of the aurora was determined as the density increase between 100-200 km altitudes according to the EISCAT radar data. The presence of the polar cap patches was determined as a strong density increase above 200 km altitude. We consider mainly the winter time because the EISCAT radar works most often in winter season. In general we identified about 150 different cases for 2010-2017 years when the data from the EISCAT 42m radar was available, however, in this paper we present only typical examples. The presented conclusions are valid for the common picture. The preliminary analyze was done in the proceeding paper [Belakhovsky et al., 2019].

3.1. Dayside/cusp precipitations

Example of the dayside precipitations on 9 January 2016 is shown on Figure 1. It was geomagnetically quite period (SYM-H = -10 nT), solar wind speed has moderate values (V = 460 km/s). At time intervals 04-08 UT and 12-14 UT it is seen the ionosphere density increase at altitudes 100-200 km associated with the charge particle precipitation according to the

https://doi.org/10.5194/angeo-2020-93
Preprint. Discussion started: 21 January 2021


Annales Geophysicae Discussions

EISCAT 42m data (MLT = UT + 3). The increase of the aurora intensity in 557.7 nm emission line measured by the NYA all-sky imager testify about presence of the particle precipitation as well (Fig. 2.).

During this geomagnetic conditions NYA station often located near the cusp region. Cusp is a small area near noon, it reaches about 3 MLT in longitude and some degrees in latitudes. The cusp can be identified by the spectral width of reflected ionosphere signal. In the region of the cusp, an increase in the spectral width of the reflected signal is observed due to an increase in turbulence. Cusp is observed with an increase in the spectral width of the reflected signal up to 200 m/s at near noon hours. The methodic of the cusp identification with using SuperDARN data was done for example in [André et al., 2000l Pilipenko et al., 2017]. According to the SuperDARN radar observations in Hankasalmi (Figure 2) the cusp near the Svalbard was registered approximately from 08 to 12 UT. The equatorial boundary of the cusp was located at 78 degrees of geographic latitudes and higher. The growth of the aurora intensity in 630.0 nm emission lines at 07-09 UT during low intensity in 557.7 nm may also testify about the optical identification of the cusp.

The different colors on panels 2-5 (Figure 1) is a projections of different GPS satellites into the ionosphere. The GPS phase scintillation index reaches the value about 0.4-0.5 radian. Possibly the jumps in phase index variations in time interval 08-11 UT may testify about the passing of the station near the cusp. There is no strong Ne increase below 200 km, testifying about the particle precipitation, according to the EISCAT 42m data at 08-11.30 UT. At the moment of the passing under the cusp region the VTEC (up to 12 TECU), ROT (up to 5 TECU/min) increase was also observed (Figure 1).

The growth of the phase index was seen not during all period of Ne enhancement (100-200 km) measured by the EISCAT radar. Possibly it's due to the field of view of EISCAT radar not coincides with the field of view of GPS receivers. So for small-scale and medium-scale Ne increase is not always correlate with phase index growth.

The ROT variations have small disturbances (2-4 TECU/min) during the presence of the particle precipitation. Amplitudes scintillation index have no distinct response to the morning and daytime precipitations.

It was not observed substorm disturbances during this day. It is seen small amplitude Pc5 pulsations (10-20 nT) in X-component of the geomagnetic field at NYA stations during morning precipitations. These Pc5 pulsations can have contribution to the charge particle precipitation into the ionosphere [Belakhovsky et al., 2016].

3.2. Substorm precipitation

The example of the substorm precipitation and the GPS scintillations response to it is shown in Figure 3 (11 December 2015). It was observed two substorms during this day. The first one was at 15.30-17.00 UT, the second was at 20.00-22.00 UT. It was polar substorms because it mainly observed at latitude higher than 70º. It can be noticed that the amplitude of the first substorm reaches the value about 1400 nT at Hornsund (HOR) station, at NYA station the amplitude of the substorm was 600 nT. The second substorm was has lower amplitude than first substorm (600 nT at HOR station). These substorms was observed without geomagnetic storm (SYM-H ≈ - 10 nT), however the solar wind speed was quite high (V = 640-680 km/s) according to the OMNI database (data not shown).

https://doi.org/10.5194/angeo-2020-93
Preprint. Discussion started: 21 January 2021


Annales Geophysicae Discussions

The ionosphere plasma density increases during substorm on more that order from $9 \cdot 10^4$ to $1 \cdot 10^6$ cm^{-3} at altitudes 100-160 km. The substorms were accompanied by the strong increase of aurora intensity in different spectrum lines. The growth of the phase scintillation index was accompanied by the appearance of the bright aurora arc according to LYR all-sky camera observations (Figure 4) oriented approximately in east-west direction.

The phase index reaches the value about 2 radians during the first substorm. The growth of the phase scintillation index was seen mainly during the substorm expansion phase (30-40 minutes). During the second substorm the phase scintillation index has the lower value (0.5-1.5 radians). The growth of the phase scintillation index was seen as sharp increases during 5-10 minutes time intervals.

Substorms do not lead to significant TEC increase. It is seen the absence of the TEC data during the substorm. It testifies about the cycle slips of GPS signal at this moment.

The ULF waves in Pi3 frequency range embedded into the substorm structure can have contribution into the particle acceleration into the ionosphere, growth of the field-aligned currents (FAC) which leads to such strong values of the phase scintillation index.

3.3. Polar cap patches

Nighttime polar cap patches. The example of the evening-nighttime polar cap patches (PCP) is shown on Figure 5 for the 10 February 2015. The PCP was observed at 19.00-23.30 UT as a density increase above 200 km according to the EISCAT data. At NYA GPS receiver the phase scintillation index reaches the medium value (0.4 radians). However the ROT variations for the PCP reach the high values (10-15 TECU/min).

During the PCP appearance the Bz-component of IMF has negative values (-6 nT) during 3 hours (data not shown). It leads to the development of the small substorm. The amplitude of the substorm is 120-140 nT in X-component of the geomagnetic field at NYA station. The PCP is also identified in the aurora intensity variations as forms propagating from the polar to low latitudes in 630.0 nm (red line) emission (Figure 7) at 19.00-23.00 UT according to LYR all-sky camera observations.

It was done the comparison of the PCP development on EISCAT 42m radar (Svalbard) and UHF radar located at lower latitudes, in Tromsø (Figure 6). The sharp increase of the plasma density (Figure 6) from 12 to 17 UT above 200 km is caused by the sunlight. At latitudes of SKN (TRO) stations the PCP manifests itself as a long lasting substorm (more than 4 hours duration) with the amplitude 200-250 nT. At SKN station the phase scintillation index has approximately the same values (0.4-0.5 radians) as in polar latitudes (NYA station).

Daytime polar cap patches. It was also analyzed the influence of GPS signals scintillations the polar cap patches propagating on the dayside. The typical example is event on 7 November 2013. It was CIR (corotating interaction region) geomagnetic storm conditions, the SYM-H index reached the value about -55 nT. According to the ionosphere plasma

https://doi.org/10.5194/angeo-2020-93
Preprint. Discussion started: 21 January 2021


Annales Geophysicae Discussions

density measurements on EISCAT 42m radar the PCPes were registered in time interval 06.00-12.00 UT (09-15 MLT) – Figure 8. The negative bay on geomagnetic field variations with amplitude about 200 nT seen on NYA station.

During this event the strong GPS phase scintillations (0.8 radians) was registered in whole time interval of the PCP appearance. Amplitude S4 index have no any clear response.

It was observed VTEC increase (from 12 to 25 TECU) caused by the PCP contribution. ROT variations have high values (7-10 TECU/min).

[Jin et al., 2017] investigated the GPS scintillations around cusp region and found that cusp precipitation has stronger influence on GPS phase scintillation when it combined with the PCP. Our analyses also confirm this finding. The event on 9 January 2016 (Figure 1) was without PCP while event on 7 November 2013 (Figure 8) was accompanied by PCP.

For the all of the considered PCP cases phase index has the value less than 1.

3.4. Precipitations associated with the interplanetary shock arrival

It is also considered the example of the interplanetary shock influence on scintillations of GPS signals. Here the example for the event of 22 January 2012 is presented. It is well known that the interplanetary shock interaction with the Earth's magnetosphere leads to strong particle precipitation into the ionosphere and leads to the appearance of the so named shock-aurora [Zhou et al., 2003]. In the paper [Belakhovsky et al., 2016] it is shown that shock wave arrival leads to the global TEC increase at high latitudes up to 40%.

The considered interplanetary shock is accompanied by an abrupt increase of the solar wind velocity (from 320 to 400 km/s), density (from 20 to 40 cm^{-3}), temperature, module of the interplanetary magnetic field (from 12 to 25 nT) according to the OMNI database, abrupt growth of the SYM-H index at 06.10 UT (Figure 9). The NYA station at the moment of interplanetary shock arrival was located on the morning side (09 MLT). For the SSC event the phase index reaches the value near about 0.3-0.4 radians (Figure 10). The ROT reaches the value about 4 TECU/min. So SSC event does not lead to the strong GPS scintillations. After the beginning of the geomagnetic storm it is seen from the EISCAT 42m radar data the development of the PCP which leads to the GPS phase scintillations (0.8 radians).

For the considered interplanetary shock cases the phase index reaches similar values (less than 1 radian).

4. Discussion

The high-latitude ionosphere is a very dynamic structure due to the charge particles (mainly electrons and protons) penetrating from the outer space which can lead to the appearance of the different times-scale ionosphere irregularities. Variations of the ionospheric electron density cause variable group delay and phase advance of the radio wave, resulting in rapid phase fluctuations or phase scintillation. The scintillation of the GPS radio signal is caused by refraction and

https://doi.org/10.5194/angeo-2020-93
Preprint. Discussion started: 21 January 2021

diffraction of radio waves passing through ionospheric irregularities on scales from tens of meters to a few kilometers [Basu et al., 1998; Kintner et al., 2007].

There are a lot of disturbances at polar ionosphere. The main phenomena are substorm and polar cap patches. In this work it is considered the influence of different types of the high latitude ionosphere disturbances (such us dayside/cusp precipitation, substorms, nighttime and daytime polar cap patches, interplanetary shock wave) on perturbations of GPS signals with using GPS scintillation receiver on Svalbard. For some events also SKN GPS scintillation receiver on mainland (Norway) was used. In this study we try to do some statistical investigation concerning the degree of influence of PCP, substorms of GPS signals disturbances. Here we present only typical events.

Concerning amplitude GPS scintillations at high latitudes we confirm the previous findings and did not found any certain reaction of the S4 index to the considered disturbances. However [Jin, 2018] have found S4 scintillations for the very strong geomagnetic storm on 17 March 2017. But it was extreme event. For the ordinary events S4 index at high latitudes haven't great increases. Possibly low values of amplitude scintillations at high latitudes are caused by the low elevation angles of GPS satellites at these regions.

The analysis shows that the polar substorms even if it observed without polar cap patches lead to the maximum values of the phase scintillation index (1.5-2 radians). From one side it is obvious because the substorm is a most powerful disturbance in the magnetosphere-ionosphere system. The ULF waves (Pi3 pulsations) embedded into substorm can accelerate electron along the field lines and produce auroral arcs. The durations of the substorm are about 1.5-3 hours while the growth of the phase scintillation index was observed during 30-40 minute (expansion phase). So the substorm leads to the high but short-time growth of the phase index. In paper [Kim, 2014] it is shown that ULF waves in Pi2 frequency range can have a dominant role in producing accelerated auroral electrons. During the substorms bright and discrete auroral forms are appeared on the sky. Such inhomogeneous ionization structures produce significant changes in the refractive index and enhance the phase scintillation index [Hosokawa, 2014]. In addition, field-aligned currents, produced field-aligned irregularities, can be the major driver of high-latitude ionospheric irregularities [Prikryl et al., 2011].

The phase scintillations are typically produced by variations in the refractive index due to ionospheric irregularities of the scale from a few kilometers to a few tens of kilometers [Kintner et al. 2007]. The phase scintillations during the substorm interval were produced through the refractive process caused by large-scale density irregularities associated with rapidly moving auroral arc. Hosokawa et al. [2014] found that phase scintillation was enhanced in relation to substorm onset and decreased as the aurora became more diffuse. They suggested that discrete aurora in the GPS signal path is necessary for the occurrence of phase scintillation during substorm intervals. In addition to scintillation, other effects such as loss of lock [Smith et al., 2008] and cycle slips [Prikryl et al., 2010] have been directly observed in relation to auroral emissions.

Polar cap patches are the source of decameter to kilometer-scale irregularities causing scintillation. In some of the considered cases the polar cap patches was observed during 6 hours on EISCAT 42m radar. Analysis shows that PCPs are accompanied by the lower values of phase index than during a substorm but this growth is registered during longer time intervals. At the same time the PCP leads to the substantially higher values of the ROT variations. ROT is the time rate of change of the

https://doi.org/10.5194/angeo-2020-93
Preprint. Discussion started: 21 January 2021

differential carrier phases, it providing information about scale size of the electron density irregularities scale which produces GPS signal scintillations. We used in our study 1-minute ROT time resolution. The typical velocity of the plasma convection at high latitudes is between 100 m/s and 1 km/s. So 1-minute ROT variations are caused by the irregularities with the scale about 6-60 km. Our observations suggest that the substorms and PCPs, being different types of the high-latitude disturbances, lead to the development of different types and scales of ionospheric irregularities.

Comparison of the EISCAT observations on Svalbard and in Tromso shows that PCP manifest itself at lower latitudes as typical substorm which produce quite comparable phase scintillations at high (Tromso) and polar (Svalbard) latitudes.

There are two plasma instabilities which can explain the ionospheric irregularities at high latitudes: the gradient drift instability (GDI) and the Kelvin–Helmholtz instability (KHI). The GDI requires a density gradient and it can produce irregularities at the trailing edge of a plasma patch, while the KHI requires a velocity shear and the irregularities can be created around boundaries of velocity shears. The GDI can work on these sharp density gradients very efficiently [Moen et al., 2013] to produce small-scale irregularities which cause scintillations. The polar cap patches represent the largest scale structure in the high latitude ionosphere. During their convection in the polar cap, the Gradient Drift Instability (GDI) acts on them and develops small scale irregularities on the trailing edge.

It was done in our study the identifications of the cusp regions with using the SuperDARN ionosphere reflected signals and optical data. Cusp region is a source of the plasma turbulence of the different scales. It is found the medium growth of the TEC, ROT near the cusp region. Cusp phase scintillations are lower than dayside PCP scintillations. On the dayside, the cusp is an active region of the GPS scintillation [Moen et al., 2013], where loss of signal locks is known to occur [Oksavik et al., 2015]. By analyzing GPS phase scintillation around magnetic noon, it is suggested that GPS phase scintillations are sensitive to a combination of the cusp aurora and the intake of solar EUV-ionized plasma [Jin et al., 2015].

The common analysis shows that in all of the considered events we observed significant phase scintillations. PCPs lead to the prolonged variations of phase index but with smaller values (less than 1). Shock induced precipitation, daytime and cusp precipitation leads to the medium values of phase index (0.4-0.5 radians) and not high values of the ROT. But among the all types of the disturbances the substorms leads to the greatest values of the phase scintillations index. Thus, the substorm precipitation has the strongest impact on the scintillation of GPS radio signals in the polar ionosphere even without PCP. Substorm leads to short-time (10-20 minute) and strongest values of GPS phase scintillations while PCP to long-time (some hours) medium values of GPS phase scintillations. So both types of these ionosphere disturbances are dangerous for the quality of communications, navigations, and locations at polar latitudes.

5. Conclusions

It is considered the influence of different types of the high latitude ionosphere disturbances (such us daytime/cusp precipitations, substorms, nighttime and daytime polar cap patches, interplanetary shock wave) on perturbations of GPS

https://doi.org/10.5194/angeo-2020-93
Preprint. Discussion started: 21 January 2021


Annales Geophysicae Discussions Open Access EGU

signals with using receivers on Svalbard and in Skibotn. All of the considering types of the ionospheric disturbances leads to the growth of phase scintillations index and ROT variations.

Substorms (even without PCP) lead to the maximum values of the phase scintillation index (1.5-2 radians). The growth of the phase index observed mainly during the substorm expansion phase. ULF waves in Pi3 frequency range during a substorm producing auroral arcs can lead to such high values of the phase index.

Polar cap patches lead to the prolonged variations of phase index with smaller values (less than 1). At the same time polar cap patches can lead to strong ROT variations (10-15 TECU/min) in comparison with the substorms disturbances. So our observations suggest that the substorms and PCPs, being different types of the high-latitude disturbances, lead to the development of different types and scales of ionospheric irregularities.

Cusp region, indentified with using SuperDARN radar, leads to the moderate growth of phase scintillation index, TEC ROT variations. Shock induced precipitations leads to medium values of the phase scintillation index (0.4-0.5 radians), and medium values of the ROT (4-6 TECU/min). Our analyses show no clear response of the amplitude GPS scintillation index to the different types of the ionosphere disturbances.

Code and data availability. The authors thank the Norwegian Polar Research Institute at Ny-Ålesund for assisting us with the GPS receiver in Ny-Ålesund, Bjørn Lybekk and Espen Trondsen for the instrument operations. The IMF data are provided by the NASA OMNI Web service (http://omniwegsfc.nasa.gov).

The authors wish to thank IMAGE (http://www.ava.fmi.fi/image/), EISCAT groups for the available data. EISCAT is an international association supported by research organizations in China (CRIRP), Finland (SA), Japan (NIPR and STEL), Norway (NFR), Sweden (VR), and the United Kingdom (NERC). Data from EISCAT can be obtained from the Madrigal database http://www.eiscat.se/madrigal. The University of Oslo ASI data are available at http://tid.uio.no/plasma/aurora.

The authors acknowledge the use of SuperDARN data. SuperDARN is a collection of radars funded by national scientific funding agencies of Australia, Canada, China, France, Italy, Japan, Norway, South Africa, United Kingdom and the United States of America.

Author contributions. VB take a part in formulation of the problem, analyze events, do conclusions, and write text with contributions from all the co-authors. YJ take a part in formulation of the problem, process GPS, optical data, correct text. WM take a part in formulation of the problem, organize this research team.

Competing interests. The authors declare that they have no conflict of interest.

Acknowledgements. This work is supported by the Russian Science Foundation (grant # 18-77-10018).

https://doi.org/10.5194/angeo-2020-93
Preprint. Discussion started: 21 January 2021

Annales Geophysicae Discussions

References

Alfonsi L., Spogli L., De Franceschi G., Romano V., Aquino M., Dodson A. and Mitchell C. N.: Bipolar climatology of GPS ionospheric scintillation at solar minimum, Radio Science, 46, RS0D05, https://doi.org/10.1029/2010RS004571. 2011.

André R., Pinnock M., Rodger A. S.: Identification of the low-altitude cusp by Super Dual Auroral Radar Network radars: A physical explanation for the empirically derived signature, Journal of Geophys. Res., Vol. 105, № 12, P. 27081-27094, https://doi.org/10.1029/2000JA900071, 2000.

Basu S., Groves K. M., Basu S. and Sultan P.J.: Specification and forecasting of scintillations in communication/navigation links: Current status and future plans, Journal of Atmospheric and Solar-Terrestrial Physics, 64 (16), 1745–1754, https://doi.org/10.1016/S1364-6826(02)00124-4, 2002.

Belakhovsky V., Pilipenko V., Murr D., Fedorov E., Kozlovsky A.: Modulation of the ionosphere by Pc5 waves observed simultaneously by GPS/TEC and EISCAT, Earth, Planets and Space, Vol. 68., article id.102, https://doi.org/10.1186/s40623-016-0480-7, 2016.

Belakhovsky V.B., Pilipenko V.A., Sakharov Ya.A., Lorentzen D.L., Samsonov S.N.: Geomagnetic and ionospheric response to the interplanetary shock on January 24, 2012, Earth, Planets and Space, Vol. 69, Issue 1, article id. #105., https://doi.org/10.1186/s40623-017-0696-1, 2017.

Belakhovsky V. B., Jin Y., Miloch W. J.: Influence of Different Ionospheric Disturbances on the GPS Scintillations at High Latitudes, Springer Proceedings in Earth and Environmental Sciences, Problems of Geocosmos–2018, P. 281-287. https://doi.org/10.1007/978-3-030-21788-4_24, 2020.

Carrano C. S., Anghel A., Quinn R.A., and Groves K.M.: Kalman filter estimation of plasmaspheric total electron content using GPS, Radio Science, 44, RS0A10, https://doi.org/10.1029/2008RS004070, 2009.

Clausen L. B. N., Moen J. I., Hosokawa K., Holmes J. M.: GPS scintillations in the high latitudes during periods of dayside and nightside reconnection, J. Geophys. Res., 121, 3293–3309, https://doi.org/10.1002/2015JA022199, 2016.

Crowley G., Ridley A. J., Deist D., Wing S., Knipp D. J., Emery B. A., Foster J., Heelis R., Hairston M., and Reinisch B. W.: Transformation of high-latitude ionospheric F region patches into blobs during the March 21, 1990, storm, J. Geophys. Res., 105, A3, 5215–5230, https://doi.org/10.1029/1999JA900357, 2000.

Foster J.C., Coster A.J., Erickson P.J., Holt J.M., Lind F.D., Rideout W., McCready M., A. van Eyken, Barnes R.J., Greenwald R.A., Rich F.J.: Multiradar observations of the polar tongue of ionization, J. Geophys. Res., 110, A09S31, https://doi.org/10.1029/2004JA010928, 2005.

Hosokawa K., Shiokawa K., Otsuka Y., Nakajima A., Ogawa T., and Kelly J. D.: Estimating drift velocity of polar cap patches with all-sky airglow imager at Resolute Bay, Canada, Geophysycal Research Letters, 33, L15111, https://doi.org/10.1029/2006GL026916, 2006.

Hosokawa K., Otsuka Yu., Ogawa Y. and Tsugawa T.: Observations of GPS scintillation during an isolated auroral substorm, Progress in Earth and Planetary Science, 1:16, https://doi.org/10.1186/2197-4284-1-16, 2014. Jin Y., Moen J.,

https://doi.org/10.5194/angeo-2020-93
Preprint. Discussion started: 21 January 2021

Miloch W.: GPS scintillation effects associated with polar cap patches and substorm auroral activity: direct comparison, Journal of Space Weather and Space Climate, 4, A23, https://doi.org/10.1051/swsc/2014019, 2014.

Jin Y., Moen J. I., and Miloch W. J.: On the collocation of the cusp aurora and the GPS phase scintillation: A statistical study, J. Geophys. Res., 120, 9176–9191, https://doi.org/10.1002/2015JA021449, 2015.

Jin Y., Moen J. I., Miloch W. J., Clausen L. B. N., and Oksavik K.: Statistical study of the GNSS phase scintillation associated with two types of auroral blobs, J. Geophys. Res., 121, 4679–4697, https://doi.org/10.1002/2016JA022613, 2016.

Jin Y., Moen J. I., Oksavik K., Spicher A., Clausen L. B.N., Miloch W. J. GPS scintillations associated with cusp dynamics and polar cap patches: J. Space Weather Space Clim., 7, A23. https://doi.org/10.1051/swsc/2017022, 2017.

Jin Y., Oksavik K. GPS scintillations and losses of signal lock at high latitudes during the 2015 St. Patrick's Day storm: J. Geophys. Res., 123, 7943–7957, https://doi.org/10.1029/2018JA025933, 2018.

Kim H., Clauer C.R., Deshpande K., Lessard M.R., Weatherwax A.T., Bust G.S., Crowley G., Humphreys T.E.: Ionospheric irregularities during a substorm event: Observations of ULF pulsations and GPS scintillations, Journal of Atmospheric and Solar-Terrestrial Physics, 114, 1–8, http://dx.doi.org/10.1016/j.jastp.2014.03.006, 2014.

Kinrade J., Mitchell C.N., Smith N.D., Ebihara Y., Weatherwax A.T., and Bust G.S.: GPS phase scintillation associated with optical auroral emissions: First statistical results from the geographic South Pole, J. Geophys. Res., 118, 2490–2502, https://doi.org/10.1002/jgra.50214, 2013.

Kintner P. M., Ledvina B. M., and De Paula E. R.: GPS and ionospheric scintillations, Space Weather, 5, S09003, https://doi.org/10.1029/2006SW000260, 2007.

Lockwood M., and Carlson Jr. H. C.: Production of polar cap electron density patches by transient magnetopause reconnection, Geophys. Res. Lett., 19, 1731–1734, https://doi.org/10.1029/92GL01993, 1992.

Lorentzen D. A., Moen J., Oksavik K., Sigernes F., Saito Y., and Johnsen M. G.: In situ measurement of a newly created polar cap patch, J. Geophys. Res., 115, A12323, https://doi.org/10.1029/2010JA015710, 2010.

Moen J., Oksavik K., Alfonsi L., Daabakk Y., Romano V., and Spogli L.: Space weather challenges of the polar cap ionosphere, J. Space Weather and Space Clim., 3, A02, https://doi.org/ 10.1051/swsc/2013025, 2013.

Oksavik K., Moen J., Lester M., Bekkeng T.A., and Bekkeng J. K.: In situ measurements of plasma irregularity growth in the cusp ionosphere, J. Geophys. Res., 117, A11301, https://doi.org/10.1029/2012JA017835, 2012.

Oksavik K., Van der Meeren C., Lorentzen D.A., Baddeley L.J., and Moen J.: Scintillation and loss of signal lock from poleward moving auroral forms in the cusp ionosphere, J. Geophys. Res., 120, 9161–9175, https://doi.org/10.1002/2015JA021528, 2015.

Pilipenko V., Belakhovsky V., Engebretson M. J., Kozlovsky A., Yeoman T.: Are dayside long-period pulsations related to the cusp?, Ann. Geophys., 33, P. 395-404, https://doi.org/10.5194/angeo-33-395-2015, 2015.

Prikryl P., Jayachandran P. T., Mushini S. C., Pokhotelov D., MacDougall J.W., Donovan E., Spanswick E., St.-Maurice J.-P.: GPS TEC, scintillation and cycle slips observed at high latitudes during solar minimum, Ann. Geophys., 28, 1307–1316, https://doi.org/10.5194/angeo-28-1307-2010, 2010.

https://doi.org/10.5194/angeo-2020-93
Preprint. Discussion started: 21 January 2021

Prikryl P., Jayachandran P.T., Mushini S.C., Chadwick R.: Climatology of GPS phase scintillation and HF radar backscatter for the high-latitude ionosphere under solar minimum conditions, Ann. Geophys., 29, 377–392, https://doi.org/10.5194/angeo-29-377-2011, 2011.

Rostoker G., Akasofu S.-I., Foster J., Greenwald R., Kamide Y., Kawasaki K., Lui A., McPherron R., and Russel C.: Magnetospheric substorms-definition and signatures, J. Geophys. Res., 85(A4), 1663–1668, https://doi.org/10.1029/JA085iA04p01663, 1980.

Smith A.M., Mitchell C.N., Watson R.J., Meggs R.W., Kintner P. M., Kauristie K., Honary F.: GPS scintillation in the high arctic associated with an auroral arc, Space weather, vol. 6, s03d01, https://doi.org/10.1029/2007SW000349, 2008.

Van Dierendonck A.J., Klobuchar J., Hua Q.: Ionospheric Scintillation Monitoring Using Commercial Single Frequency C/A Code Receivers. Paper presented at Proceedings of the 6th International Technical Meeting of the Satellite Division of The Institute of Navigation (ION GPS 1993), Salt Lake City, UT, September 22–24, 1993.

Van der Meeren C., Oksavik K., Lorentzen D., Moen J. I., Romano V.: GPS scintillation and irregularities at the front of an ionization tongue in the nightside polar ionosphere, J. Geophys. Res., 119, 8624–8636, https://doi.org/10.1002/2014JA020114, 2014.

Van der Meeren C., Oksavik K., Lorentzen D.A., Rietveld M.T., and Clausen L.B.N.: Severe and localized GNSS scintillation at the poleward edge of the nightside auroral oval during intense substorm aurora // J. Geophys. Res., 120, 10,607–10,621, https://doi.org/10.1002/2015JA021819, 2015.

Van der Meeren C., Oksavik K., Lorentzen D. A., Paxton L.J., Clausen L.B. N. Scintillation and irregularities from the nightside part of a Sun-aligned polar cap arc, J. Geophys. Res., 121, 5723–5736, https://doi.org/10.1002/2016JA022708, 2016.

Zhang Q.-H., Zhang B.-C., Moen J., Lockwood M., McCrea I.W., Yang H.-G., Hu H.-Q., Liu R.-Y., Zhang S.-R., Lester M.: Polar cap patch segmentation of the tongue of ionization in the morning convection cell, Geophys. Res. Lett., 40, 2918–2922, https://doi.org/10.1002/grl.50616, 2013.

Zhou X.-Y., Strangeway R.J., Anderson P.C., Sibeck D.G., Tsurutani B.T., Haerendel G., Frey H.U., Arballo J.K.: Shock aurora: FAST and DMSP observation, J. Geophys. Res., 108:8019, https://doi.org/10.1029/2002JA009701, 2003.

https://doi.org/10.5194/angeo-2020-93
Preprint. Discussion started: 21 January 2021

Annales Geophysicae Discussions
Open Access
EGU

435

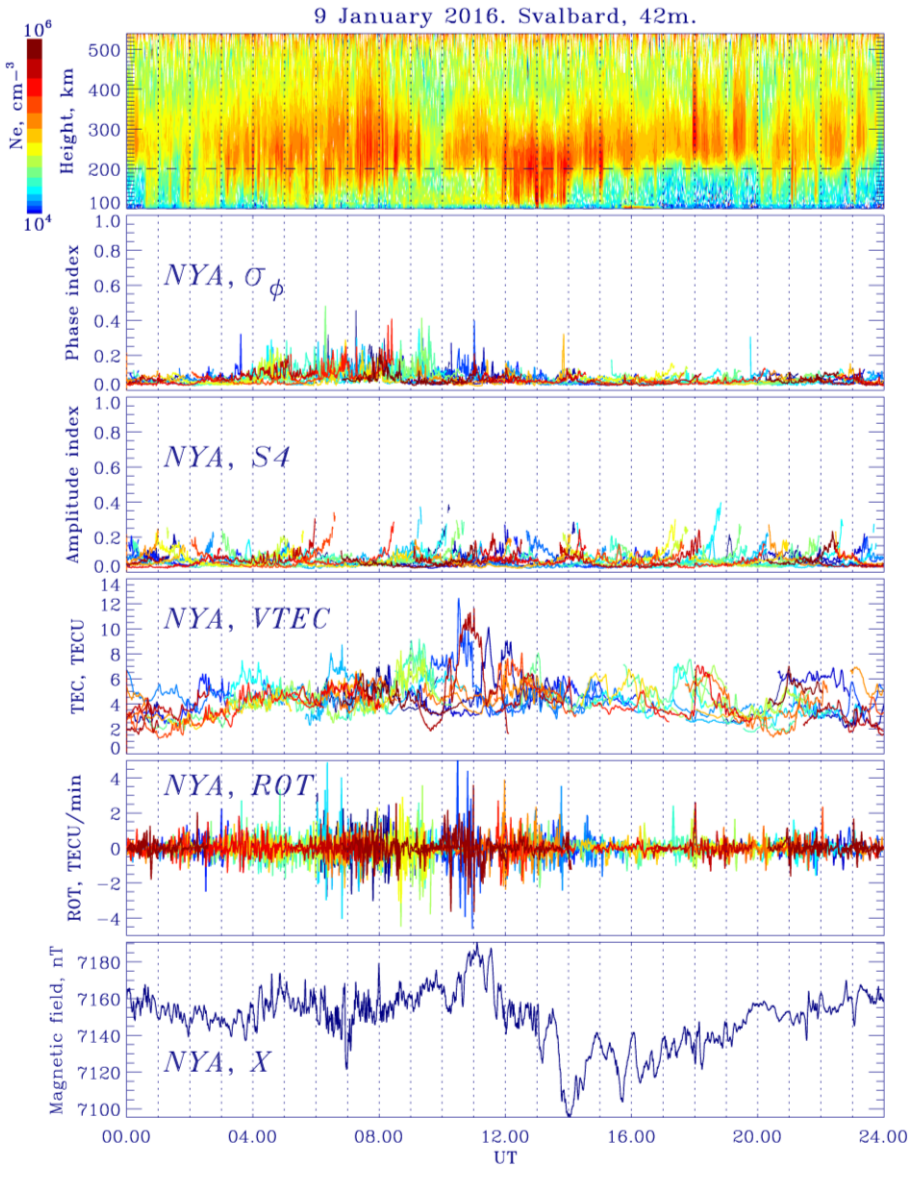

Figure 1: Ionosphere plasma density according to the EISCAT 42m radar data; phase scintillation index and amplitude scintillation index according to the GPS receiver at NYA station; TEC and ROT variations according to the GPS receiver at NYA station; geomagnetic field variations (X-component) at NYA station for the 9 January 2016.

440

https://doi.org/10.5194/angeo-2020-93
Preprint. Discussion started: 21 January 2021

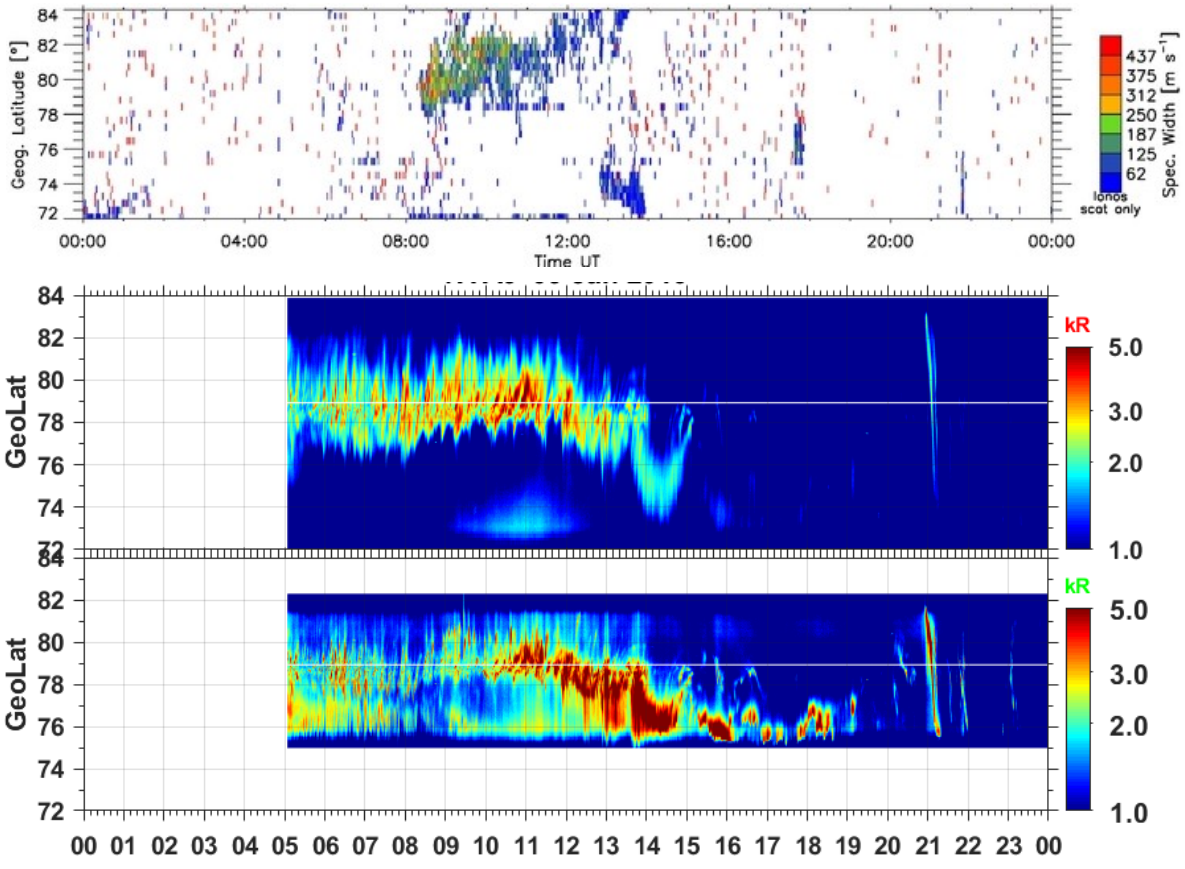

Figure 2: Latitude-time plot of the spectral width according SuperDARN Hankasalmi radar, keograms (557.7 nm and 630.0 nm emission line) from the all-sky imager at NYA station for the 9 January 2016.

https://doi.org/10.5194/angeo-2020-93
Preprint. Discussion started: 21 January 2021

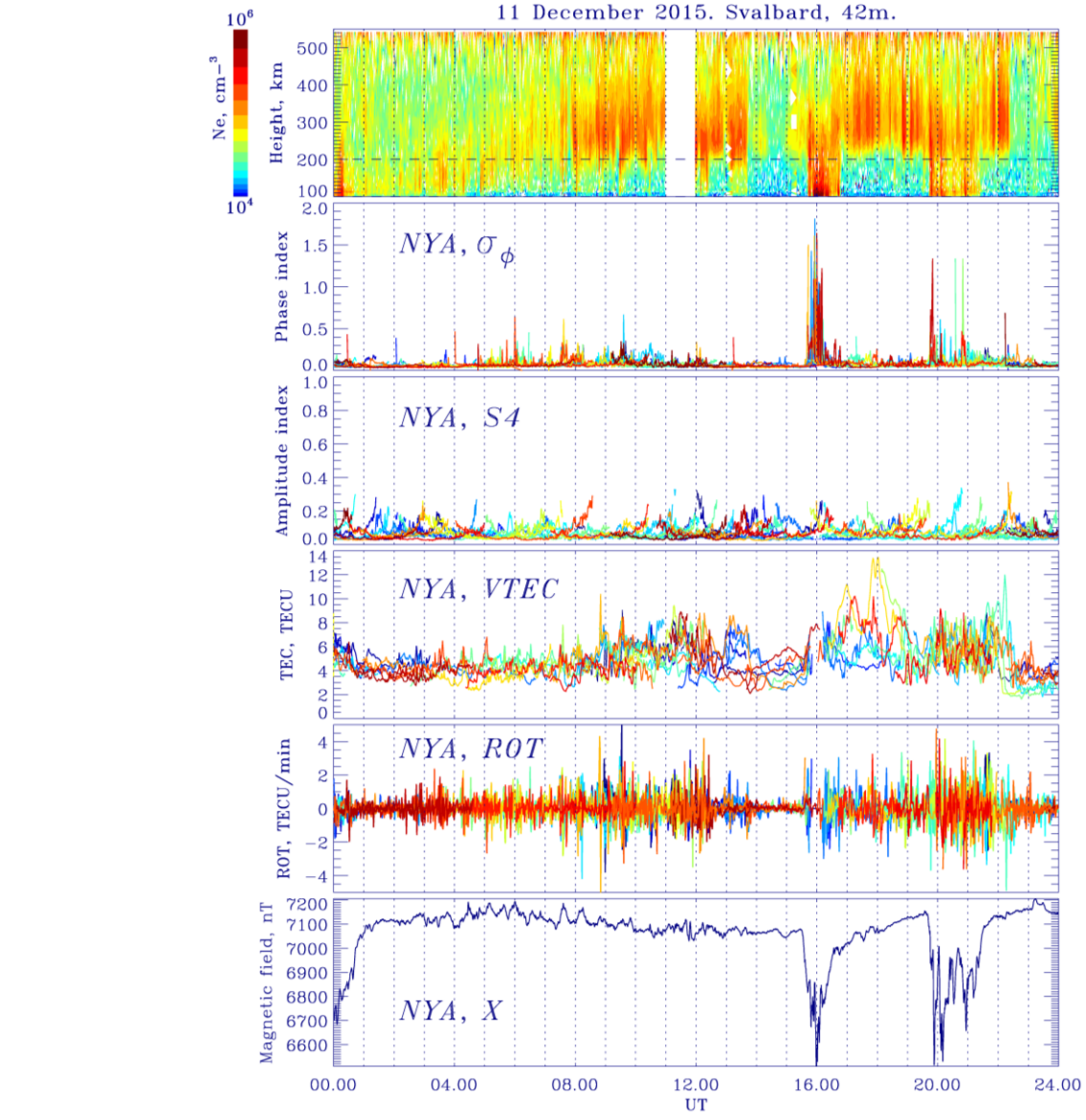

Figure 3: Ionosphere plasma density according to the EISCAT 42m radar data; phase scintillation index and amplitude scintillation index according to the GPS receiver at NYA station; TEC and ROT variations according to the GPS receiver at NYA station; geomagnetic field variations (X-component) at NYA station for the 11 December 2015.

https://doi.org/10.5194/angeo-2020-93
Preprint. Discussion started: 21 January 2021

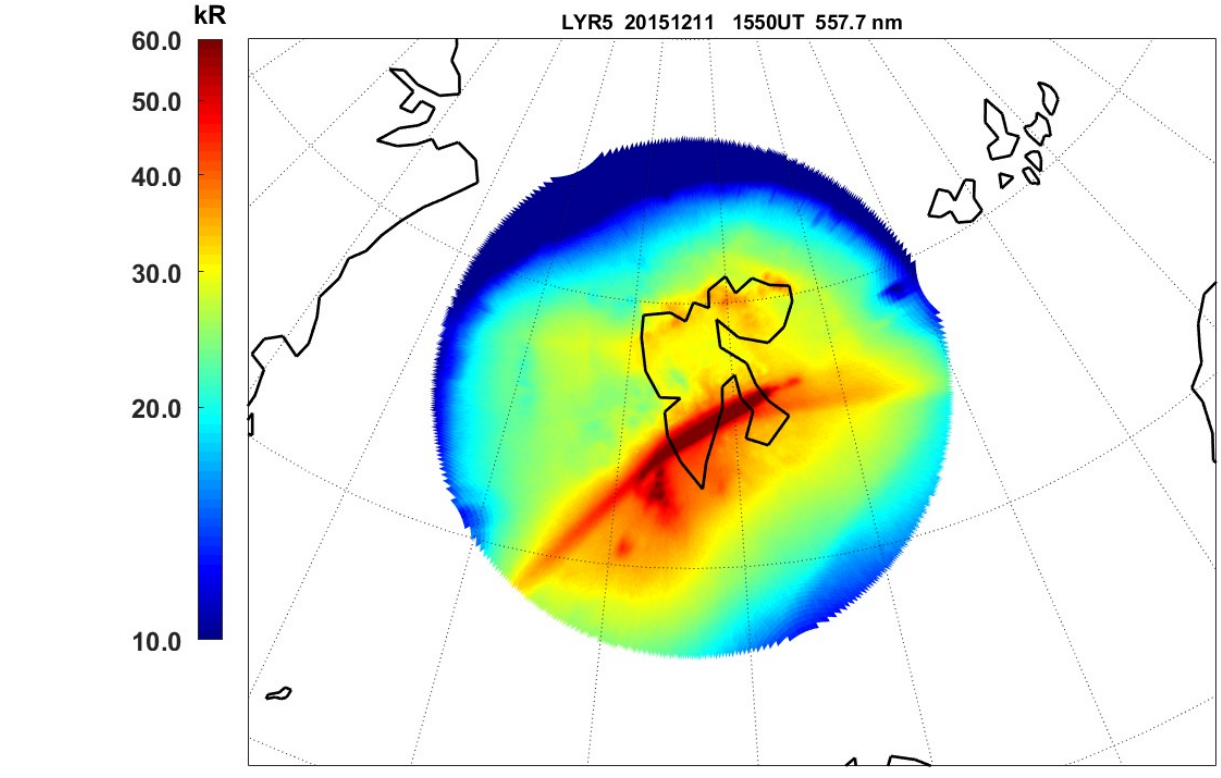

Figure 4: The all-sky camera image (557.7 nm emission) at LYR station projected into the map for the 15.50 UT 11 December 2015.

https://doi.org/10.5194/angeo-2020-93
Preprint. Discussion started: 21 January 2021

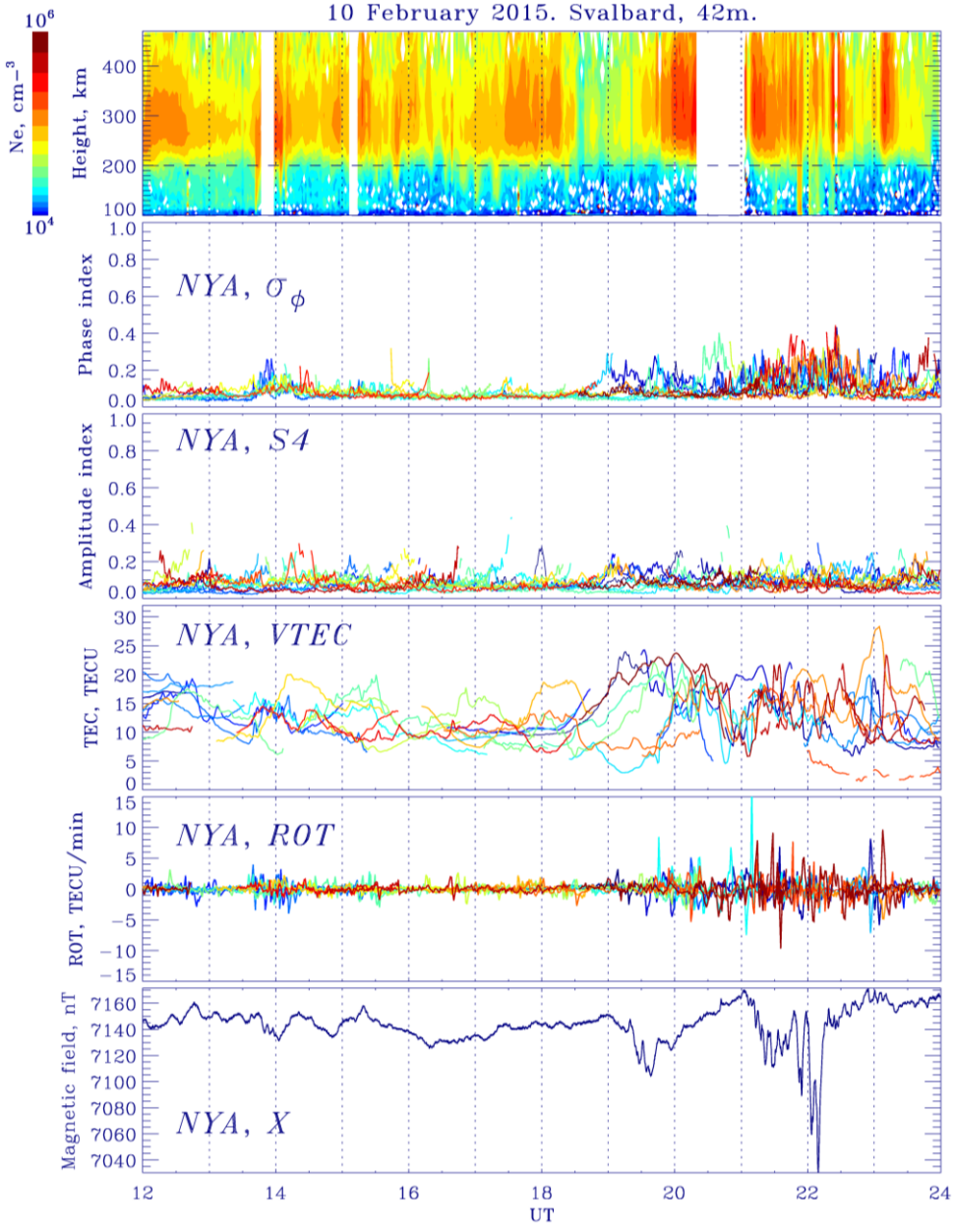

490 **Figure 5: Ionosphere plasma density according to the EISCAT 42m radar data; phase scintillation index and amplitude scintillation index according to the GPS receiver at NYA station; TEC and ROT variations according to the GPS receiver at NYA station; geomagnetic field variations (X-component) at NYA station for the 10 February 2015.**

https://doi.org/10.5194/angeo-2020-93
Preprint. Discussion started: 21 January 2021

Annales Geophysicae Discussions
Open Access
EGU

495

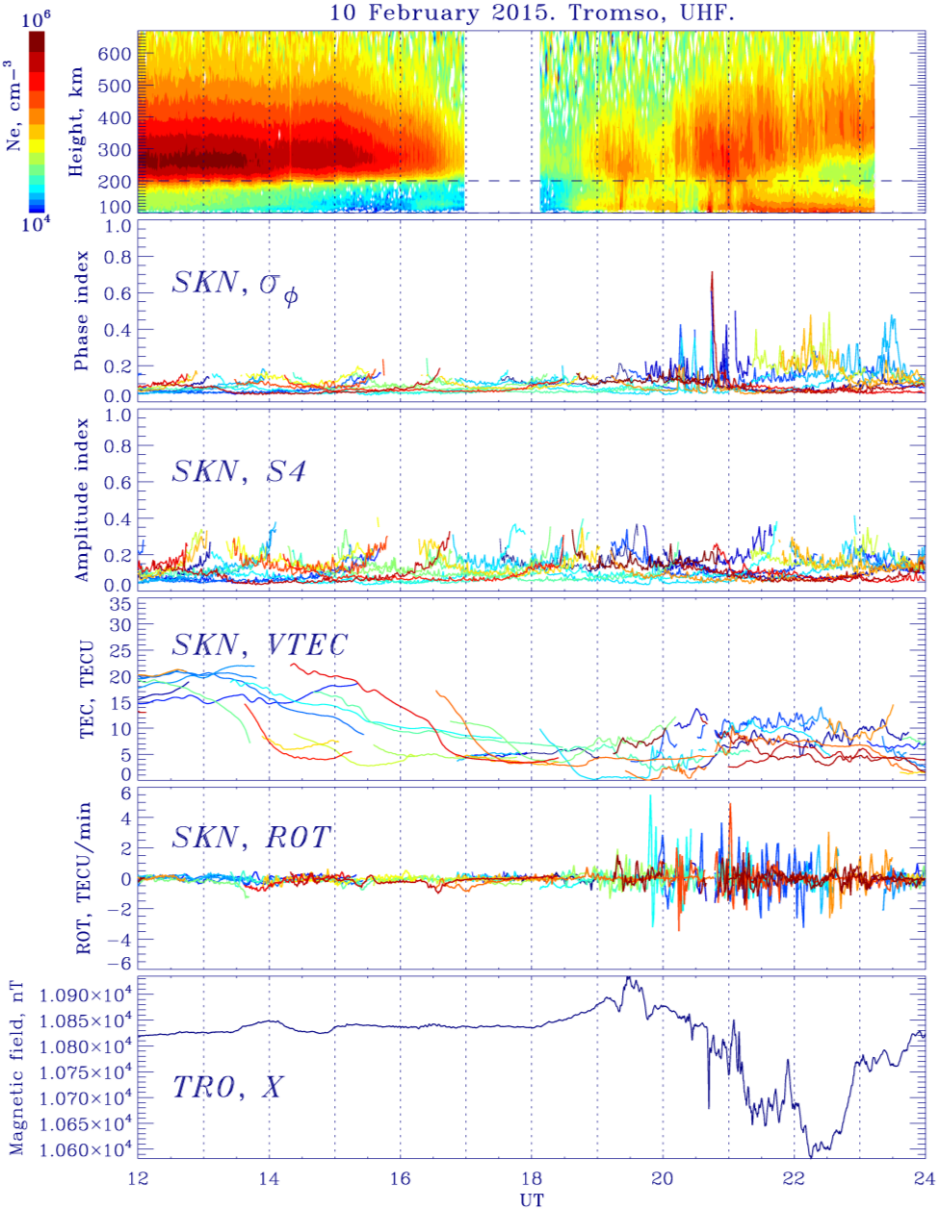

Figure 6: Ionosphere plasma density according to the UHF EISCAT radar data; phase scintillation index and amplitude scintillation index according to the GPS receiver at SKN station; TEC and ROT variations according to the GPS receiver at SKN station; geomagnetic field variations (X-component) at TRO station for the 10 February 2015.

500

https://doi.org/10.5194/angeo-2020-93
Preprint. Discussion started: 21 January 2021

Annales Geophysicae Discussions
Open Access
EGU

505

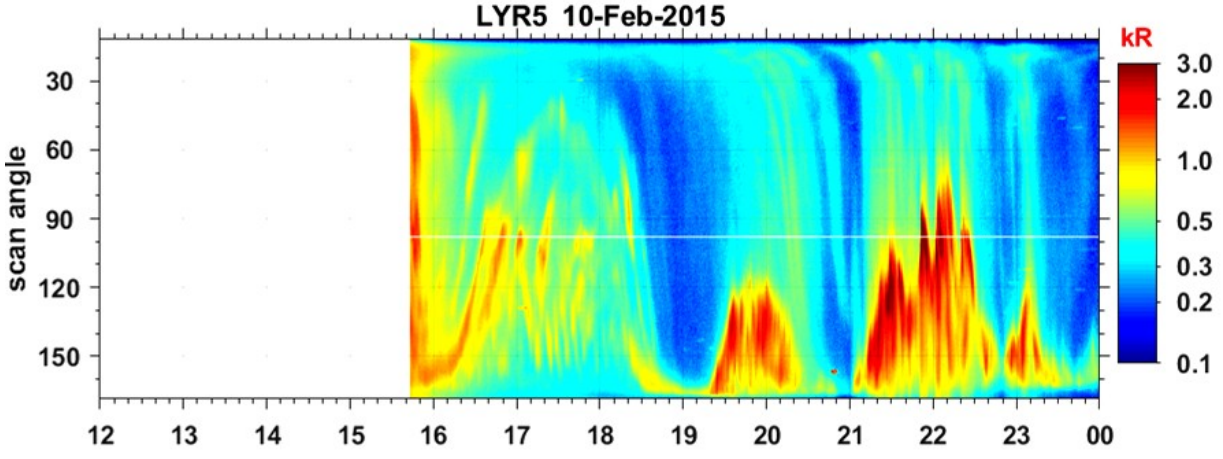

510

Figure 7: Keogram (630.0 nm emission line) from the all-sky imager at LYR station for the 10 February 2015.

515

520

https://doi.org/10.5194/angeo-2020-93
Preprint. Discussion started: 21 January 2021

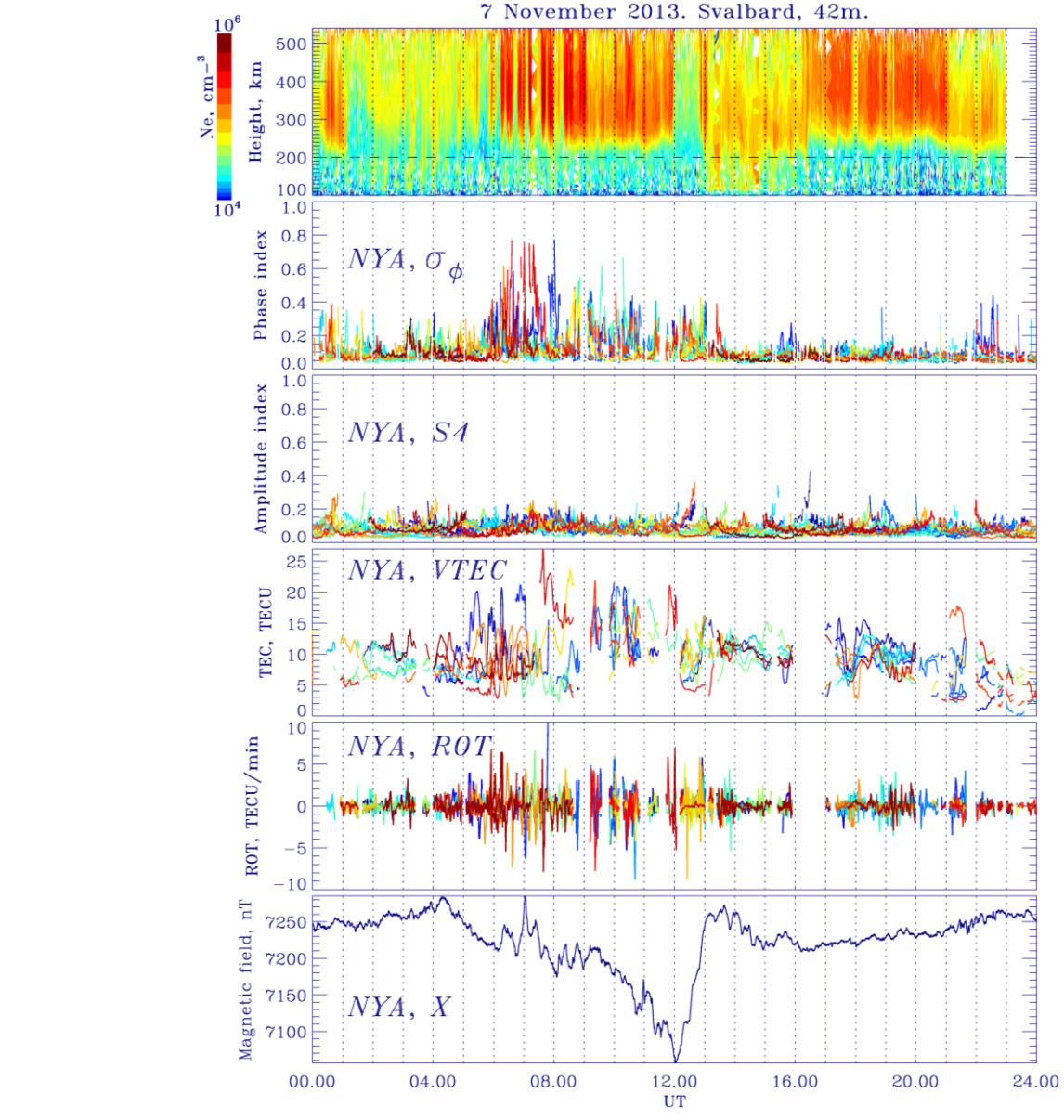

Figure 8: Ionosphere plasma density according to the EISCAT 42m radar data; phase scintillation index and amplitude scintillation index according to the GPS receiver at NYA station; TEC and ROT variations according to the GPS receiver at NYA station; geomagnetic field variations (X-component) at NYA station for the 7 November 2013.

https://doi.org/10.5194/angeo-2020-93
Preprint. Discussion started: 21 January 2021

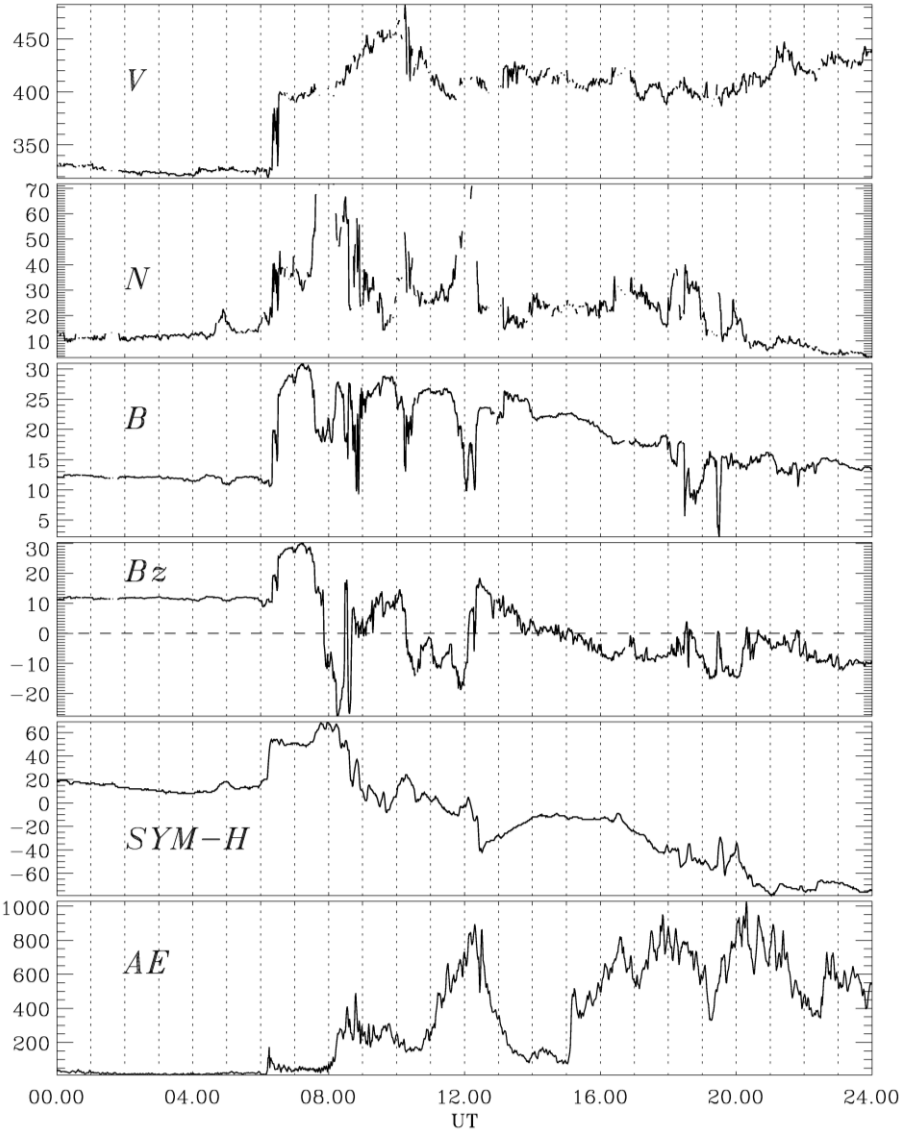

Figure 9: Solar wind speed V [km/s], solar wind density N [cm-3], module of the IMF B [nT], Bz-component [nT] of IMF according to the OMNI database, SYM-H index [nT], AE index [nT] for the 22 January 2012.

https://doi.org/10.5194/angeo-2020-93
Preprint. Discussion started: 21 January 2021

Annales Geophysicae Discussions

540

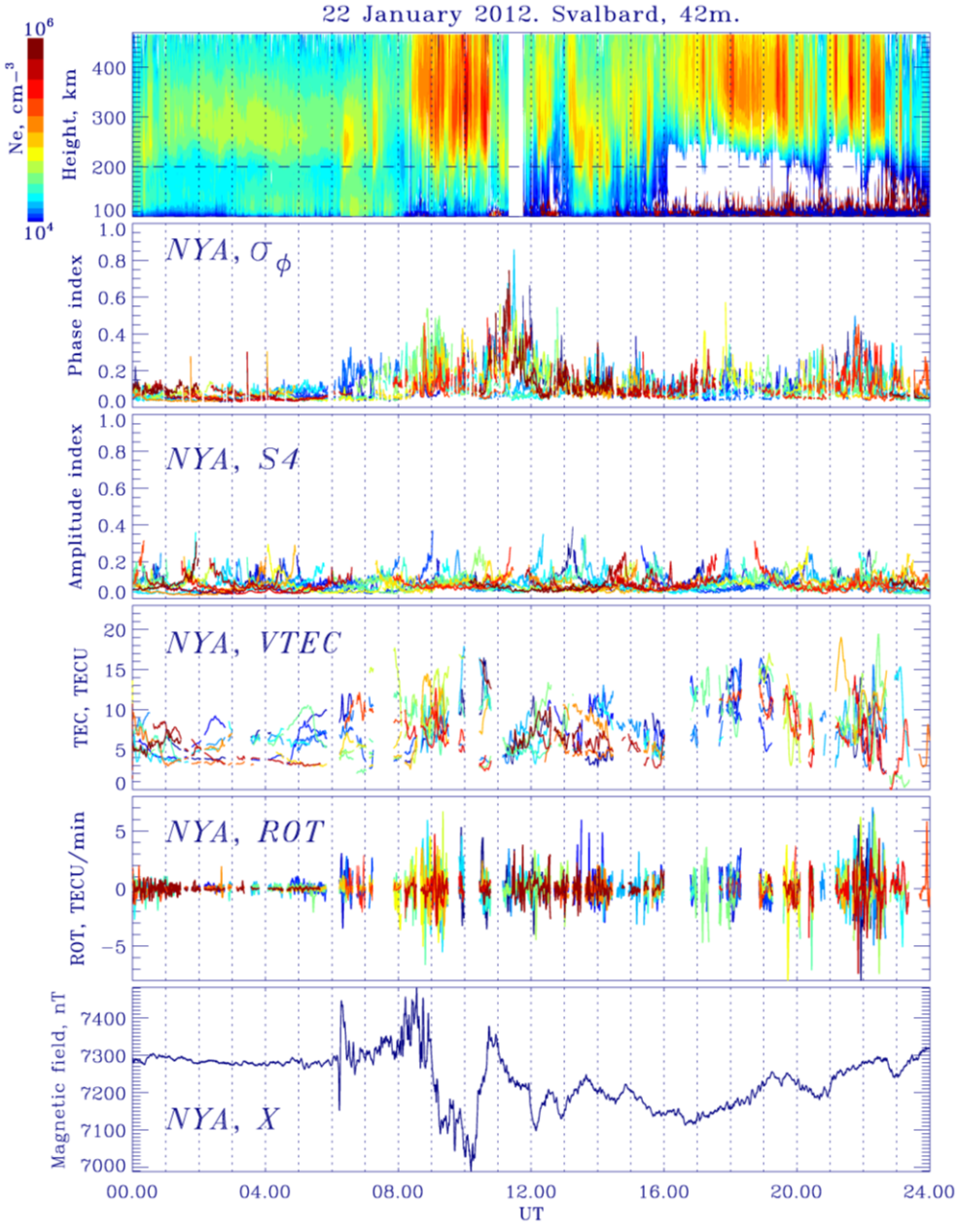

Figure 10: Ionosphere plasma density according to the EISCAT 42m radar data; phase scintillation index and amplitude scintillation index according to the GPS receiver at NYA station; TEC and ROT variations according to the GPS receiver at NYA station; geomagnetic field variations (X-component) at NYA station for the 22 January 2012.